First-Pass Radionuclide Angiography Using a Multiwire Gamma Camera and Tantalum-178

Jeffrey L. Lacy, Mario S. Verani, Mark E. Ball, Terri M. Boyce, Robert W. Gibson, and Robert Roberts

Section of Cardiology, Department of Medicine, Baylor College of Medicine, The Methodist Hospital, Houston, Texas

A portable multiwire gamma camera (MWGC) with enhanced imaging characteristics relative to conventional sodium iodide camera has been evaluated with ^{178}Ta, a short-lived, generator-produced radioisotope (half-life 9.3 min). First-pass radionuclide angiography (FPRA) was performed and results were compared to those obtained with FPRA using a multicrystal camera (MCC) and ^{99m}Tc in 38 patients. The overall left ventricular count sensitivity (counts/mCi/sec/millisteradians [msr]) was significantly higher with MWGC/^{178}Ta (176 ± 132 versus 108 ± 49, p < 0.001) yielding images of higher statistics with higher resolution collimation (31 versus 63 msr). Left ventricular ejection fraction was 0.54 ± 0.18 by MWGC and 0.54 ± 0.18 by MCC with an excellent correlation between the two techniques (r = 0.94, s.e.e. = 0.06). The detection of wall motion abnormality was virtually identical with the two techniques. Intra- and interobserver reproducibility by MWGC was excellent (r = 0.99 and 0.99, respectively). Thus, this new technology provides first-pass studies of higher statistical quality and improved resolution, affording more precise assessment of left ventricular performance and likelihood of further substantial improvement by use of even higher doses of ^{178}Ta.

Conventional gamma cameras utilize sodium iodide crystals for detection of radiation. Two distinct types of cameras are employed: single crystal and multicrystal cameras. In the single crystal devices, count rate is limited by pulse pileup to ~150,000 cps (*1*). This limitation in count rate hinders adequate cardiac first-pass imaging, a technique which has many virtues (*2,3*). Single crystal cameras also have large intrinsic image nonuniformities requiring correction circuitry and frequent surveillance for drift (*4*). Multicrystal gamma cameras (MCC) possess improved count-rate capability but have relatively poorer spatial resolution (1 cm), imposed by the size of their individual crystal elements (*5,6*). The large size and heavy weight of single and multicrystal cameras discourage their use in acutely ill patients and preclude close coupling of two or more detectors. To minimize these limitations we have developed a camera employing a multiwire proportional

detector rather than sodium iodide (*7,8*). The inherent imaging characteristics of the multiwire gamma camera (MWGC), including spatial resolution, count-rate performance, and image uniformity, are superior to those of both single and multicrystal sodium iodide devices (*8*). The MWGC is extremely light and very portable as well as amenable to coupling of multiple detectors for multiview imaging. Conventional cardiac imaging is also hampered by the relatively long half-life of the commonly used isotope, technetium (^{99m}Tc), which gives prolonged radiation exposure and hinders utilization for frequent, repetitive first-pass imaging. The MWGC operating at moderate pressurization is ideally suited for use with tantalum (^{178}Ta), a low-energy (60 keV), short-lived (half-life = 9.3 min) isotope. This short half-life, which is 30 times shorter than that of ^{99m}Tc, provides substantially reduced radiation dose and improved image statistics as a result of larger injectable doses. Since ^{178}Ta is generator produced (*9–11*) from the parent tungsten (^{178}W), it can be conveniently utilized in clinical work.

To assess the clinical performance of this new cam

era-isotope combination, studies were performed in 38 patients. First-pass left ventricular (LV) radionuclide angiography performed with the MWGC using [178]Ta was compared to conventional first-pass radionuclide angiography performed with ^{99m}Tc and the MCC.

MATERIALS AND METHODS

Study Design and Patient Population

Patients referred to the Nuclear Cardiology Laboratory for assessment of ventricular function by radionuclide angiography were randomly selected for the study. The protocol was approved by the Baylor College of Medicine and The Methodist Hospital Institutional Review Boards for Human Research. All patients were required to sign an informed consent. A total of 38 patients were studied, comprised of 23 men and 15 women ranging in age from 35 to 84 yr (mean 60 ± 12 yr). Patient weights ranged from 95 to 267 lb (mean 170 ± 37 lb). The majority of patients (27 or 71%) had coronary artery disease documented by coronary arteriography. Six patients had had a previous myocardial infarction. Nine other patients had peripheral vascular disease and two patients with previous cerebral vascular accident had no demonstrable cardiovascular disease. First-pass radionuclide angiography was performed in order to assess the left ventricular function in those patients.

Each patient was studied first by the MWGC/[178]Ta and then by the Baird System Seventy-Seven MCC/^{99m}Tc technique. Thirty to forty-five minutes between studies was allowed to ensure that levels of [178]Ta during the MCC study were reduced by an order of magnitude, compared to the injected ^{99m}Tc dose.

Multiwire Gamma Camera

The portable MWGC is shown in Figure 1. Its characteristics and design have been described in detail previously (8). The instrument utilizes a uniquely designed high speed delay line readout system (7) which provides digital position measurements at very high rates while at the same time providing intrinsic resolution and field uniformity (expressed as standard deviation about the mean) superior to available commercial technology as outlined in Table 1. A conventional lead hexagonal hole collimator was employed with an opening solid angle of 31 msr. The holes of this unit are 0.178 cm wide by 0.94 cm long and the septal thickness is 0.018 cm.

Multicrystal Gamma Camera

The Baird System Seventy-Seven with 294 sodium iodide crystals of dimension 1 × 1 cm² arranged in a grid of 14 × 21 elements, has been described elsewhere (5). The peak count rate of the device is 400,000 cps. A 1-in.-thick collimator with a 63 msr opening solid angle was utilized. A new version of this camera has recently been introduced. The characteristics of this device are very similar to the System Seventy-Seven with the exception that a higher count rate is provided. This improved specification would have little effect on the results of this study since clinical doses of [99m]Tc (~20 mCi) do not tax the System Seventy-Seven count rate capability (6).

Tantalum-178 Generator

The [178]Ta generator employed with the MWGC has been described in detail elsewhere (12). The generator is based upon previously reported chemistry (11) but incorporates

FIGURE 1
Multiwire gamma camera with subject positioned for clinical study.

modifications which substantially improve breakthrough and yield performance as well as convenience and safety in clinical application. This generator has been approved by the Food and Drug Administration for investigational use.

First-Pass Imaging Technique

All studies were performed in the anterior projection with the subjects in an upright position. The isotope was injected through a 1¼-in., 18-gauge Teflon catheter inserted into a medial antecubital vein. The radioisotope, either [178]Ta or ^{99m}Tc, was loaded into an extension tube of 2 ml capacity, connected to the catheter, and flushed in by hand with 25 to 30 ml of saline at ~8 ml/sec. In order to investigate the effects of variable [178]Ta dose level on count rate and image quality, the full available dose was injected. Since each generator was utilized for a period of 4 wk, the dose varied over a wide range

TABLE 1
Intrinsic Imaging Characteristics of the Multiwire Gamma Camera

Peak count rate	850,000 cps
Spatial resolution	2.5 mm
Image uniformity	±5%
Active area	25 cm diameter
Weight	23 kg
External dimensions	40 × 40 × 12 cm

of 13 to 53 mCi. The standard ^{99m}Tc dose of 15 to 20 mCi (mean 19 mCi) was utilized. For both studies, data collection was begun just prior to injection and continued for 30 sec. A frame duration of 25 msec was employed. For the MWGC studies, a $32 \times 32 \times 16$ image matrix (0.75 cm/pixel) and a 30% energy window around the 60-keV peak of ^{178}Ta was employed. Data were acquired directly on hard disk and archived to streamer tape. The MCC studies employed the standard $14 \times 21 \times 8$ matrix (1.1 cm/pixel) and 30% energy window around the 140 keV peak of ^{99m}Tc. Data were acquired on hard disk and archived on magnetic tape.

Data Processing

Data processing for the MCC/^{99m}Tc studies was performed on the Baird System Seventy-Seven computer to obtain LV representative cycle images, time-activity curve (TAC), and ejection fraction (EF) (12–14).

Processing of the MWGC/^{178}Ta studies was performed utilizing a dedicated DEC LSI 11/23 computer which also performed data acquisition. Specialized software was developed for this purpose. This software performs the following processing steps.

1. All end-diastole frames recorded during the study are located utilizing the digitized ECG signal recorded during image acquisition. Each end-diastolic frame is averaged together with its two preceding and two succeeding frames. This averaged frame is then nine point filtered and displayed on a screen for the entire study (Fig. 2).

2. The operator then draws approximate LV and right ventricular (RV) regions of interest on two of these frames and the TAC for these regions is formed and displayed at the bottom of this same screen.

3. The operator then selects the dominant LV beats by moving a cursor to the desired end-diastole frame and pressing a select button. As the cursor is moved from frame to frame, a marker is automatically positioned along the TAC curves at the bottom of the screen indicating the LV and RV activity for that particular end-diastole frame. Left ventricular beats are included if their activity at end-diastole is >70% of the maximal LV activity at end-diastole. The computer then combines the selected LV beats to form a single representative cycle image sequence and applies a spatial (2-4-2 convolution) filter.

4. The lung background beat is selected as the minimum point of the LV-TAC. End-systolic frames on both sides of this end-diastolic frame are then displayed and the operator selects the one with minimal RV content. The lung background frame is then formed by adding the same number of frames about this end-systolic frame as the number of LV beats selected. This lung background frame must be multiplied by a scale factor <1 to correct for the washout from lung to LV phase. To quantify the washout, a lung region of interest (LROI) is defined as that region outside of the LV region in the lung background frame whose count is above 30% of the maximum extraventricular count. The ratio of LROI counts in the end-diastolic LV frame to those in the lung background frame reflects the lung background activity remaining during the LV phase. The lung background frame is multiplied by this ratio and the resulting frame is subtracted from all frames of the representative LV cycle.

5. To aid in locating the valve plane, pixels in which activity increases from end-diastole to end-systole are then flagged on the representative cycle end-diastole frame and this image is blown up to a 64×64 matrix and displayed on the screen. The accurate LV region is then outlined on this frame by following the border of the flagged region in the valve plane area and along the 30% isocontour in other areas.

6. The final LV-TAC is then obtained using this region. This curve and the corresponding representative cycle images are then scaled throughout the diastolic phase. The scaling rigorously corrects for varying activity dilution resulting from the fact that during diastole, blood with lower radionuclide activity relative to that remaining from the last systole is entering the ventricle. Each point in the diastolic phase (C_t) is corrected by:

$$C_t' = \frac{C_{beg\ syst}}{C_{end\ diast}} \cdot \frac{C_t - C_{end\ syst}}{C_{end\ diast} - C_{end\ syst}},$$

where C_t' is the scaled counts, $C_{beg\ syst}$ is counts at beginning of systole; C_t is the original counts before scaling; $C_{end\ diast}$ is counts at end-diastole and $C_{end\ syst}$ is counts at end-systole. Thus, counts at end-systole are unchanged while counts at end-diastole are scaled to equal the counts at the onset of systole. This curve is then filtered by 2-4-2 convolution.

7. A flow curve is computed by differentiating the TAC curve and plotting it along with the TAC curve.

8. The EF is computed from the end-diastole and end-systole points in the TAC, as: EF = (end-diastolic counts − end-systolic counts)/end-diastolic counts.

9. The end-diastole LV border is overlaid on all frames of the representative cycle images to aid in cinematic assessment of wall motion.

This processing sequence typically requires <5 min to

FIGURE 2
Sequential images consisting of nine point filtered average of five frames, corresponding in time to end-diastole for every cardiac cycle recorded during a study. The LV and RV region of interest histograms computed from these end-diastolic frames are shown on the bottom left and bottom right, respectively.

complete by an experienced operator, is free from subjective operator decisions, and incorporates important quality control feedback by providing continuous image assessment during background selection.

The distinctions between this software and that of the MCC are the following.

1. In the MCC analysis, the operator selects the background frame based only on the LV-TAC with no information of RV-TAC and without ready access to the selected background image.

2. No ECG data are encoded or utilized by the MCC in determining end-diastolic frames. These frames are located by the computer from the LV-TAC.

3. The EF is computed prior to representative cycle generation by locating successive peak and valley points on the LV-TAC and summing the counts to obtain end-diastole and end-systole counts. After background subtraction, these values are utilized to compute EF.

4. The MCC utilizes a backward filling procedure to correct the diastole phase of the TAC but does not perform a true dilution correction.

5. The frames of the MCC studies are multiplied up by a constant provided by the manufacturer to correct for the camera's acquisition deadtime. This maneuver results in artifactually higher count rates and is not necessary since the background frame is scaled by the count-ratio between lung phase and LV phase which automatically corrects for deadtime variation.

Wall Motion Analysis

Wall motion analysis was performed by one experienced observer who had no clinical information about the patients. The MWGC and MCC studies were interpreted at least 1 week apart. The wall motion in these studies was graded on a semiquantitative point scale, where 3 denoted normal motion, 2 moderate hypokinesis, 1 severe hypokinesis, 0 akinesis, and −1 dyskinesis. The walls analyzed were the anterolateral, apical, and inferior walls in the anterior projection. The MWGC studies were seen in closed-loop cinematic display on a Ramtek color display. The MCC studies also were viewed in cinematic format on a 12-in. TV screen

Statistical Analysis

Data are presented as mean ± s.d. Linear regression analyses were done for comparison between techniques. Student's paired t-tests were used to compare differences between two techniques. A p value of <0.05 was considered significant.

RESULTS

Ejection Fraction: Comparison of MWGC with MCC

The individual values for the EF determined by MWGC and MCC are listed in Table 2. The mean LV-EF was 0.54 ± 0.18 (range 0.07 to 0.85) by MCC and 0.54 ± 0.18 (range 0.08 to 0.88) by MWGC (p = N.S.). Linear regression analysis between the MCC and MWGC yielded an r of 0.94, a slope of 0.94 and a s.e.e. of 0.06 (Fig. 3). Intra and interobserver reproducibility of EF calculation by the MWGC/[178]Ta was excellent,

with correlation coefficients of 0.99 and 0.99 and s.e.e. of 0.02 and 0.03, respectively (Fig. 4).

Regional Wall Motion: Comparison Between MWGC and MCC

Left ventricular wall motion images obtained with the MWGC and [178]Ta are shown in Figure 5 for Subjects 1 through 16 (Table 2). In these images, the end-diastolic border is overlayed on the end-systolic image with 30% thresholding. Thirty patients had normal wall motion and eight had abnormal wall motion by MWGC and MCC. In the eight patients with abnormal wall motion, three patients had severe, diffuse hypokinesis by both methods; the other five patients had a total of 13 abnormal segments, 12 of which were detected by both techniques. The wall motion scores in these patients were 4.8 ± 1.5 by MWGC and 4.8 ± 1.9 by MCC (p = N.S.). One patient had mild inferobasal hypokinesis by MWGC and normal motion by MCC. All patients with abnormal wall motion or depressed (<50%) EF had coronary artery disease.

Image Count Statistics

The peak count rate for the MWGC studies is plotted versus injected [178]Ta dose in Figure 6. Linear regression analysis yielded an r of 0.91. Note that at peak count-rate no detectable saturation was observed with the MWGC. This is consistent with the measured saturation curve which peaks at 850,000 cps (8). The mean peak count-rate with no deadtime correction was 310,600 ± 125,000 for the MWGC and 147,500 ± 18,000 cps (p < 0.001) for the MCC/Tc99m.

The LV end-diastolic count statistics are listed for each patient in Table 2 including both actual end-diastolic count (EDC) per 25 msec interval and the absolute sensitivity parameter S_n, defined as EDC per mCi of injected dose per msr of collimator opening angle per second of counting interval (see Appendix). The mean values of S_n were 176 ± 132 for the MWGC and 108 ± 49 for the MCC indicating that for equivalent collimator opening angles (yielding equivalent in vivo resolution) and equal injected doses, the MWGC/[178]Ta provides higher count statistics than the MCC by a factor of 1.61. End-diastolic count was found to depend upon EF as well as injected dose. This dependence upon EF is due to slower transit of activity through the left ventricle in cases of low EF which provides a larger number of usable beats. Thus, multiparameter correlation analysis was performed to obtain the dependence of EDC on these two variables, using the relation EDC = (dose/EF) × a + b, (a, b = slope and intercept, respectively). Linear regression yielded a = 55, b = 217 and an r value of 0.91 for MWGC/[178]Ta and a = 45, b = 1771 and an r value of 0.74 for MCC/[99m]Tc. The ratio of background counts to uncorrected EDC was

TABLE 2
Count Statistics and LV-EF Comparison in 38 Patients*

Patient no.	Sex	Age (yr)	Weight (lb)	^{178}Ta dose (mCi)	^{99m}Tc dose (mCi)	EDC/25 msec		S_n (counts/sec /mCi/msr)		LV-EF	
						MWGC	MCC	MWGC	MCC	MWGC	MCC
1	M	58	175	53	17	4,391	2,792	106	105	0.73	0.71
2	M	61	180	43	18	4,400	2,850	130	101	0.68	0.62
3	M	62	170	39	19	6,435	4,639	210	155	0.52	0.45
4	F	70	151	38	18	18,516	4,550	621	161	0.15	0.22
5	F	58	115	36	19	4,571	1,496	162	50	0.56	0.64
6	F	54	137	36	17	4,937	2,509	175	94	0.63	0.63
7	M	58	174	35	21	4,169	5,430	152	165	0.63	0.51
8	F	62	194	35	19	7,155	2,543	260	85	0.23	0.25
9	M	64	156	35	20	2,643	2,803	96	89	0.65	0.69
10	M	60	190	34	20	3,529	2,469	132	79	0.69	0.63
11	M	75	210	33	20	3,152	2,669	122	85	0.61	0.53
12	M	66	171	33	22	2,917	2,522	113	73	0.54	0.64
13	F	84	95	30	17	2,878	2,268	122	85	0.63	0.58
14	M	69	217	30	18	3,847	2,750	163	97	0.52	0.66
15	F	60	163	29	18	1,488	1,685	65	60	0.67	0.74
16	F	71	108	29	18	4,807	3,686	211	130	0.50	0.46
17	M	54	199	29	19	2,236	2,930	98	98	0.60	0.67
18	F	71	115	26	18	2,488	2,430	122	86	0.88	0.85
19	M	70	183	25	18	4,862	6,049	248	214	0.30	0.31
20	F	54	135	24	18	2,446	1,850	130	65	0.54	0.75
21	M	53	189	23	18	1,176	975	65	34	0.70	0.66
22	M	35	163	22	24	1,537	8,136	297	216	0.22	0.15
23	M	45	212	22	21	3,413	3,335	198	101	0.19	0.19
24	F	63	153	21	19	1,733	2,698	105	90	0.56	0.60
25	M	42	172	20	20	1,730	3,540	110	113	0.57	0.49
26	M	45	181	19	20	2,331	2,511	156	80	0.54	0.52
27	M	40	177	18	18	1,570	2,526	111	89	0.62	0.62
28	F	61	114	17	20	2,138	3,218	160	102	0.53	0.55
29	M	57	188	17	14	3,060	5,404	229	246	0.14	0.20
30	F	85	132	17	19	10,109	6,536	757	219	0.08	0.07
31	M	68	225	16	18	1,300	1,579	103	56	0.56	0.57
32	F	44	267	16	24	1,080	3,094	86	82	0.66	0.68
33	M	81	140	16	20	1,839	3,717	146	118	0.54	0.63
34	M	59	185	15	19	2,006	4,563	170	153	0.67	0.65
35	F	78	155	14	21	1,575	3,043	143	92	0.52	0.51
36	M	58	197	14	16	1,315	2,014	120	80	0.71	0.73
37	F	37	137	14	18	1,763	2,002	160	71	0.64	0.61
38	M	46	231	14	25	1,423	2,826	129	72	0.56	0.57
Mean		60	170	26	19	3,594	3,228	176	108	0.54	0.54
± s.d.		12	37	10	2	3,087	1,477	132	49	0.18	0.18

* EDC = end-diastolic count; EF = ejection fraction; LV = left ventricular; MCC = multicrystal camera; MWGC = multiwire gamma camera.
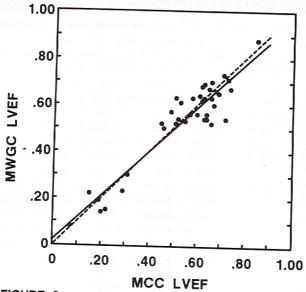
0.47 ± 0.09 for the MWGC and 0.40 ± 0.09 for the MCC studies.

In Figure 7, TAC and flow curves obtained with the two techniques are compared. Notice the fluctuations present during the peak filling phase of the MCC study of Figure 7A and during the peak ejection phase of the MCC study of Figure 7B. The curves of the MWGC have improved quality in this example. Such statistical noise in these critical regions of the curves contributes to errors when a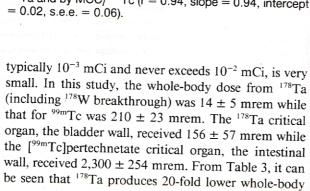ssessing important parameters such as peak ejection and filling rates and the time of their occurrence. The improved MWGC curves, as a result of higher statistics, provide more accurate assessment of these important parameters.

Patient Dosimetry

Whole-body and critical organ doses of ^{178}Ta and ^{178}W based on human and animal biodistribution are tabulated with corresponding ^{99m}Tc values (15) in Table 3. The contribution from ^{178}W breakthrough, which is

FIGURE 3

Linear regression between LV-EF determined by MWGC/^{178}Ta and by MCC/^{99m}Tc (r = 0.94, slope = 0.94, intercept = 0.02, s.e.e. = 0.06).
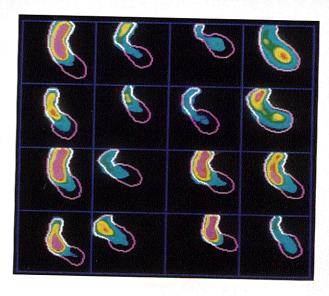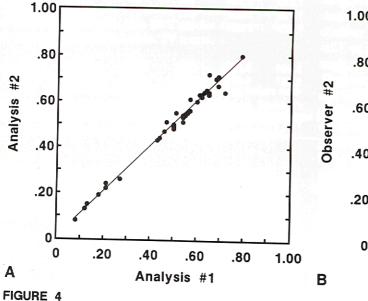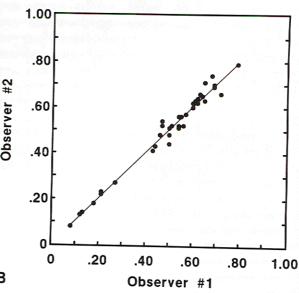

FIGURE 5

Left ventricular wall motion images (end-diastole border superimposed on end-systole image) obtained with the MWGC and ^{178}Ta. Studies 1 through 16 (Table 2) are shown left to right, top to bottom.

typically 10^{-3} mCi and never exceeds 10^{-2} mCi, is very small. In this study, the whole-body dose from ^{178}Ta (including ^{178}W breakthrough) was 14 ± 5 mrem while that for ^{99m}Tc was 210 ± 23 mrem. The ^{178}Ta critical organ, the bladder wall, received 156 ± 57 mrem while the [^{99m}Tc]pertechnetate critical organ, the intestinal wall, received 2,300 ± 254 mrem. From Table 3, it can be seen that ^{178}Ta produces 20-fold lower whole-body

and 20-fold lower critical organ exposure than a similar dose of [^{99m}Tc]pertechnetate.

Performance of the Tantalum-178 Generator

A total of six generators were employed throughout the course of this study, each utilized for a period of 4 wk. All units performed reliably for the full duration of use with very low levels of breakthrough.

FIGURE 4

Intra- (Fig. 4A) and inter- (Fig. 4B) observer correlation plots. A) r = 0.99, slope = 0.98, intercept = 0.02, s.e.e. = 0.02. B) r = 0.99, slope = 0.99, intercept = 0.01, s.e.e. = 0.03.
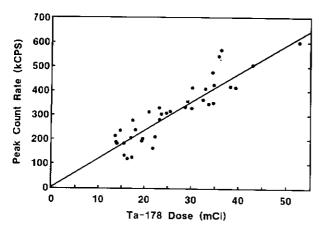
FIGURE 6
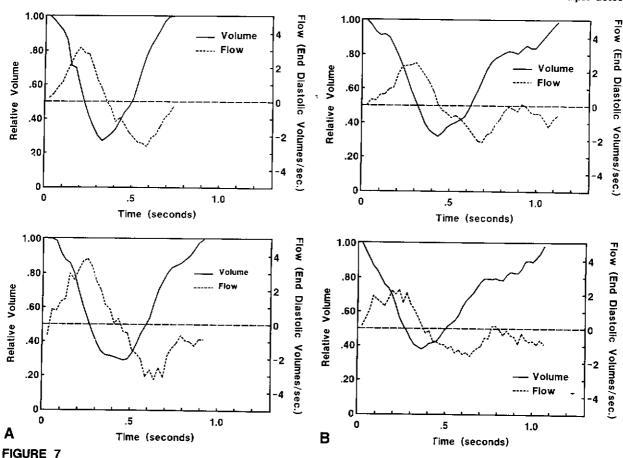Peak count rate of MWGC versus injected ^{178}Ta dose.

DISCUSSION

We applied a new gamma camera, utilizing a multi-wire proportional counter and ^{178}Ta, to perform radionuclide angiography. Studies performed in 38 patients revealed a close correlation between the EF determined by this new technique and by the best conventional first-pass technology using ^{99m}Tc and a multicrystal

TABLE 3
Adult Radiation Dosimetry ^{178}Ta/^{178}W Versus ^{99m}Tc

	Whole-body dose (mrem/mCi)	Critical organ	Critical organ dose (mrem/mCi)
^{178}Ta	0.53	Bladder wall	6.00
^{178}W	48	Bladder wall	520
^{99m}Tc pertechnetate	11	Intestinal wall	120

gamma camera (r = 0.94). Detection of abnormal wall motion also correlated very well with that of conventional first-pass angiography. Higher count-rates and image statistics were achieved with the MWGC despite much lower patient radiation dose. Our results indicate that even higher count-rates are possible with increased doses of isotope yet overall radiation dose would still be less than with ^{99m}Tc.

The MWGC camera is a highly compact and light-weight system in which the predominantly digital electronics is simpler than that of conventional gamma cameras which rely heavily on analog circuitry. The simplicity of the electronics and the detector should result in significantly lower production cost. It should be possible to construct a camera with multiple detec-

FIGURE 7
Repeated time-activity curve (solid) and flow curve (dashed) from MWGC/^{178}Ta study (top) and MCC/^{99m}Tc study in the same patient (bottom). 7A) Study No. 1 with 53 mCi ^{178}Ta and 17 mCi ^{99m}Tc; 7B) Study No. 2 with 43 mCi ^{178}Ta and 18 mCi ^{99m}Tc.

tors that would be competitive in cost with single detector sodium iodide cameras. Furthermore, because of its simple, rugged digital design, the multiwire camera is far more trouble-free than the sodium iodide cameras.

Image Count Statistics

This study shows that with the MWGC and [178]Ta the image count statistics are substantially improved over conventional techniques. The higher count-rate permits the use of higher resolution collimation which affords images of improved resolution. No saturation of the MWGC count-rate was seen with [178]Ta doses up to 53 mCi. Thus, the optimal [178]Ta dose with the collimator we used is in excess of 50 mCi. With such doses, improvement in count statistics by a factor of 3 is achieved and the patient whole body radiation dose is still reduced many fold relative to [99m]Tc. Examples of the benefits of the improved statistics are exhibited in the time activity and flow curves of Figure 7. They demonstrate that the accuracy of determination of important parameters involving count differences, such as peak ejection rate and peak filling rate, from the MCC/^{99m}Tc studies can be seriously compromised by the statistical noise present during these phases of the flow curves. In contrast, the flow curves from the MWGC/[178]Ta studies have significantly less statistical noise, providing the potential for more accurate determination of those parameters. Of course, a detailed study focusing on this area and involving many more cases is required to quantify the benefits of this improvement, but they could be substantial.

Other Potential Uses of the Multiwire Gamma Camera and Short-Lived Isotopes

An important feature of [178]Ta not assessed in this study is the potential to label other biologic markers. An effective blood label can be achieved with direct injection of [178]Ta (10). In addition to the blood pool both lung and liver agents labeled with [178]Ta have been reported and evaluated in animals (16). Lung ventilation studies utilizing commercially available aerosol systems should also be feasible.

Another promising potential isotope for use with the MWGC is the ultra-short lived iridium-191m ([191m]Ir) (half-life = 5 sec) whose dominant 65 keV x-rays can be effectively imaged (17,18). Preliminary studies with this radionuclide and the MWGC in our laboratory have indicated that high quality first-pass radionuclide angiography is feasible in the vast majority of adult patients, allowing determination of LV-EF and wall motion with extremely low radiation exposure and utilization concurrently with thallium-201 perfusion studies (19).

Clinical Implications

The vast majority of exercise radionuclide angiography is currently performed with single crystal cameras

and gated technique. There are several limitations to this technology. Imaging at the very peak of exercise—which the patient may not be able to sustain because of symptoms—is difficult to achieve due to the need for the 2 to 3 min minimal acquisition time. Chest motion at high intensity exercise can be a problem, particularly with long imaging time. And finally, perhaps the most fundamental problem is that quantitative imaging is only possible in the left anterior oblique view due to the overlap of left and right ventricle in all other views. This view is not ideal for assessment of motion in the very important anterior, apical and infero-basal ventricular walls which are the areas most affected by left anterior descending and right coronary stenoses, respectively.

The MWGC and [178]Ta provides a highly accurate, low cost technology for first-pass radionuclide angiography, which enables assessment of ventricular function at the very peak of exercise. In contrast with blood pool radionuclide angiography, quantitative imaging is feasible during exercise in any view, providing assessment of virtually all cardiac walls. Thus, this technology may become a useful tool for identifying symptomatic patients who may require further invasive testing. Moreover, it may allow screening for occult coronary artery disease in selected high risk, asymptomatic populations.

Further benefits are the possibility to perform bedside serial monitoring of cardiac function in critically ill patients, including those receiving acute interventions, such as thrombolytic therapy for acute myocardial infarction. Likewise, due to the reduced radiation dose, serial assessment of ventricular function is feasible in the long-term follow-up of individuals with coronary artery disease treated medically, surgically or by coronary angioplasty.

Another benefit of the greatly reduced radiation dose combined with the improved resolution provided by the MWGC is the quantification of shunt and ventricular function in pediatric patients. Last, given the compactness of this camera and feasibility of coupling multiple detector heads, first-pass imaging with [178]Ta could, in the future, be conveniently performed in simultaneous multiple views providing the potential for further improvement of assessment of ventricular function.

APPENDIX

Count Sensitivity Determination

The inherent sensitivity of a given camera-isotope system is evaluated by determining the counts obtained in the left ventricular region of interest at end-diastole. In order to perform accurate sensitivity comparisons with other techniques, the relative sensitivities of collimators, and variation in injected dose and framing interval employed must be taken into account. The overall sensitivity in counts per second per millicurie of a given collimator-detector combination applied

to in vivo imaging is:

$$S = \frac{\Omega}{4\pi} \, P\epsilon A \times 3.7 \times 10^7 (\text{cps/mCi}), \qquad (1)$$

where Ω = solid angle acceptance of the collimator in steradians; P = collimator packing fraction or the fraction of perpendicular incident rays that do not intersect the collimator septa; ϵ = detector efficiency; A = tissue attenuation factor. Since in vivo image resolution is proportional to the square root of the collimator acceptance opening angle, it is important to compare counts corrected for the same collimator acceptance. Thus, we define a normalized left ventriculography sensitivity parameter S_n as the number of observed counts above background at end-diastole in the left ventricular region of interest per millisecond, per mCi of injected dose and per msr of collimator acceptance solid angle. Typically the three to eight beats having maximal left ventricular activity are combined in this measurement. This parameter can be employed to compare sensitivities under conditions of equivalent in vivo resolution as determined by collimator acceptance angle. It is given by

$$S_n = \frac{EDC}{d\Omega t}, \qquad (2)$$

where EDC = the counts at end-diastole in the left ventricular region of interest, d = injected dose in mCi, t = framing interval in msec, Ω = acceptance solid angle in msr. The quantity S_n is, of course, proportional to $P\epsilon A$ as is S and thus can be expressed as:

$$S_n = kP\epsilon A, \qquad (3)$$

where the proportionality factor k contains all subject-dependent parameters other than tissue attenuation (such as cardiac output).

ACKNOWLEDGMENTS

REFERENCES

1. Lewellen TK, Murano R. A comparison of count rate parameters in gamma camera. *J Nucl Med* 1981; 22:161–168.
2. Scholz PM, Rerych SK, Moran JF, et al. Quantitative radionuclide angiography. *Cathet Cardiovasc Diagn* 1980; 6:265–283.
3. Upton MT, Rerych SK, Newman GE, et al. The reproducibility in radionuclide angiocardiographic measurements of left ventricular function in normal subjects at rest and during exercise. *Circulation* 1980; 62:126–132.
4. Abrahamson H, Brandt R, Gullquist R, Strandell T. On stability of scintillation detectors. *J Nucl Med* 1981; 22:824–826.
5. Jones RH, Grenier RP, Sabiston DC Jr. Description of a new high count rate gamma camera system. In: *Medical radioisotope scintigraphy.* International Atomic Energy Agency. 1973; SM-164/122:299–312.
6. Heyda DW, Croteau FR, Govaert JA. A third generation digital gamma camera. Proceedings of The International Society of Optical Engineering Application of Optical Instrumentation in Medicine 1984; XI:454:478–484.
7. Lacy JL, Lindsey RS. High resolution readout of multiwire proportional counters using the cathode coupled delay line technique. *Nucl Instrum Meth* 1974; 119:483–498.
8. Lacy JL, LeBlanc AD, Babich JW, et al. A gamma camera for medical applications using a multiwire proportional counter. *J Nucl Med* 1984; 256:1003–1012.
9. Holman BL, Harris GL, Neirinckx RD. Tantalum 178—a short lived nuclide for nuclear medicine: Production of the parent. *J Nucl Med* 1978; 19:510–513.
10. Babich JW, LeBlanc AD, Lacy JL, et al. Biological fate of tungsten-178 and tantalum-178. *J Nucl Med* 1983; 24:122.
11. Neirinckx RD, Jones AG, Darus MA, et al. Tantalum-178—a short lived nuclide for nuclear medicine: Development of a potential generator system. *J Nucl Med* 1978; 19:514–519.
12. Marshall RX, Berger JH, Costin JC, et al: Assessment of cardiac performance with quantitative radionuclide angiocardiography. Sequential left ventricular ejection fraction, normalized left ventricular ejection rate and regional wall motion. *Circulation* 1977; 56:820–829.
13. Nuclear cardiology reference manual for use with System Seventy-Seven. Baird Corporation, Nuclear Division, 1979:II-2.
14. Verani MS, Hartung GH, Hoepfel-Harris J, et al. Effects of exercise training on left ventricular performance and myocardial perfusion in patients with coronary artery disease. *Am J Cardiol* 1981; 47:797–803.
15. MIRD Dose Estimate Report No. 8. Summary of current radiation dose estimates to normal humans from ^{99m}Tc as sodium pertechnetate. *J Nucl Med* 1976; 17:74–77.
16. Neirinckx RD, Holmon BL, Davis MA. Tantalum-178 radiopharmaceuticals for lung and liver imaging. In: *Radiopharmaceuticals II: proceedings of the 2nd international symposium on radiopharmaceuticals.* Seattle, Washington: New York: Society of Nuclear Medicine, Inc., 1979:801–809.
17. Treves S, Cheng C, Samuel A, et al. Iridium-191m angiocardiography for the detection and quantitation of left-to-right shunting. *J Nucl Med* 1980; 21:1151–1157.
18. Heller GV, Treves ST, Parker AJ, et al. Comparison of ultra short-lived iridium-191m with technetium-99m for first pass radionuclide angiocardiographic evaluation of right and left ventricular function in adults. *J Am Coll Cardiol* 1986; 7:1295–1302.
19. Verani MS, Lacy JL, Treves S, et al. Simultaneous assessment of regional ventricular function and perfusion utilizing iridium-191m and thallium-201 during a single exercise test [Abstract]. *J Am Coll Cardiol* 1987; 9:4A.